Anomalous coarsening process of voids, steps, and denuded zones on a Si(111)7×7 surface

Y. Manassen,* N. Ramesh Rao,* I. Mukhopadhyay,* E. Ter-Ovanesyan, and Z. Olami
Department of Chemical Physics, The Weizmann Institute of Science, Rehovol 76100, Israel
(Received 31 July 1998)

Annealing a silicon surface covered with a submonolayer of *a*-Si at 600 °C gives a surface with voids that undergo a ripening process. If the uncovered surface has steps, the deposition of the growing and diffusing voids at this high temperature on the step creates a coarsening of the step. The coalescence of the voids with the step creates a denuded zone (in which the density of voids is below the average) both at the upper and the lower terraces. It is shown here that both the exact morphology and the scaling of the step width on one hand, and the density of voids near the step on the other hand, can be analyzed quantitatively. The scaling relations of the step width, the dynamic scaling of the voids, the denuded zones, and the scaling of the diffusion constant with size are shown to be interconnected. Using all these relations, it is possible to get a complete picture of all the characteristics of this anomalous diffusive coarsening phenomenon. So we prove that the void coarsening process is dominated by void diffusion and coalescence and that void diffusion is dominated by boundary vacancy diffusion. Thus the diffusive models of coarsening (described in the mean field by Lifshitz-Slyozov [I. M. Lifshitz and V. V. Slyozov, J. Phys. Chem. Solids **19**, 35 (1961); C. Wagner, Z. Elektrochem. **65**, 581 (1961)]) are nonrelevant in this case. [S1063-651X(99)02503-9]

PACS number(s): 68.35.Fx, 61.16.Ch, 61.46.+w, 82.65.Dp

I. INTRODUCTION

The growth of the scale of dynamical structures is an effect which is common to the evolution of surfaces, cracks, and islands in condensed matter and nonlinear physics. Usually such processes are induced by driving forces of various kinds, such as flux of particles, atomic diffusion, external forces, or chemical potentials. The morphology of the structures formed by such processes can be analyzed in detail to provide quantitative information on these stochastic kinetic processes. A real-space picture of such structures is of great advantage for the study of those mechanisms.

The invention of the scanning probe microscopy (SPM) techniques [3–5] with atomic resolution stimulated a great revolution in the field of surface science. The exact information on the positions of the atoms in the surface was used to verify surface structures which were observed from diffraction techniques. In complicated structures, this complementary information was essential. In the case of partly disordered surface structures, the information from SPM images is not complementary, but is unique. No alternative technique can provide detailed and local information on the structure and the dynamics of steps, defects, islands, vacancy islands (voids), locally disordered regions of the surface, and other structural features of the surface that lack translational periodicity. For example, one can study the process of growth and coarsening of islands and voids on crystalline surfaces and follow the island/void dynamics and coarsening in detail.

Several scanning tunneling microscope (STM) studies on disordered structural features were performed. For example, the STM tip was used to convert a fullerene molecule to an amorphous carbon phase, which was found to be turbostatic graphite according to the pair distribution function [6]. In a different work, the pair distribution functions were used to reach conclusions regarding the crystallization of amorphous silicon on Si(111)7×7 [7]. A slightly different example is the STM studies which characterized the disordered structure of elecrodeposited columnar gold films (a two-dimensional interface) [8] and a step in Si(001) under continuous deposition of silicon (a one-dimensional interface). In both cases, the interface correlations could provide much information on the kinetics of roughening. Another example is STM of dendritic islands [9]. The fractal dimension of these islands was found to be as expected from islands grown as a result of collisions with atoms that perform a random walk according to the diffusion-limited aggregation model (DLA).

In this work we focus on the phenomenon of the ripening of voids. There are several mechanisms for coarsening, i.e., the growth of the characteristic scale of domains of a minority phase within a majority phase. The most common one is known as Ostwald ripening [10]. It results from the tendency of islands to reduce the surface tension at their boundaries by growing, and is driven by diffusion of atoms between the islands. Examples of this type of coarsening are phase separations in a solid solution or in a solid liquid mixture, morphological changes in a solid such as the growth of pores in a porous solid (sintering), and separation of two immiscible liquids both in three and in two dimensions. All these processes coarsen according to this mechanism. The basic explanation of this phenomenon is given by a simple mean-field theory [1,2]. Extensions of this theory were successful in explaining the measured spatial correlations, deviations from circular shapes, and other features of the ripening process that could not be explained with the mean-field theory [11]. Two-dimensional measurements of coarsening using STM, where Ostwald ripening was observed, were reported in [12].

Coarsening of islands or voids on two-dimensional surfaces can be a realization of such Ostwald ripening. How-

*Present address: Department of Physics, Ben-Gurion University of the Negev, P.O. Box 653, Beer Sheva 84105, Israel.

ever, processes such as island/void coagulation resulting from islands/voids diffusion might be the dominant coarsening mechanism [13]. In this case the growth of islands/voids will occur mainly by coagulation of smaller ones. In such cases, the void/island diffusion constant which can be related to the cluster radius R, as $D \sim R^{-l}$, will cause a coarsening process that depends on time as $R = t^{\beta}$, where $\beta = (2+l)^{-1}$ [14]. The exponent l is dependent on the mechanism of diffusion: If the void movement is caused by adatom emission and absorption (evaporation condensation), the effect of a single diffusive event on the shift of the cluster center of mass is $\delta R_{\mathrm{cm}} \sim 1/R$ (which is the ratio between the radius of the missing atom and the cluster area). Hence the diffusion constant should be $D \sim R^{-1}$. However, if diffusion is related to diffusion of atoms along the void boundary, moving atoms will remain in the cluster. A movement of an atom along the boundary will move the center of mass by a smaller amount. Since the movement is orthogonal to the direction to the center of mass, we will get $\delta R_{\mathrm{cm}} \sim 1/R^{-3}$ and $D \sim R^{-3}$ [14,15]. STM measurement of the diffusion of large two-dimensional Ag clusters on Ag(100) [16] confirmed that in this case, the scaling of the diffusion constant with the size of the cluster is in agreement with the evaporation-condensation mechanism. On the other hand, measurements on coarsening of islands on metallic surfaces yield exponents which are closer to the diffusion along island boundaries [17].

In our case we discuss void motion. The diffusion constant of vacancies is expected to be much smaller than that of adatoms at a particular temperature. In Si(111)7×7 surface, the activation energy for silicon adatom diffusion is 1.3 eV [18] while for vacancy diffusion it is 3 eV [19]. Since the diffusion of a single vacancy is so much slower, there is a larger chance to observe coarsening through void migration and coalescence. We have shown in [13], both by looking at the morphology of many voids and by looking at the time evolution of the pair correlation function of the position of the voids, that they are attracted to each other and grow by coagulation. Nevertheless, it was still not clear to what extent the coagulations are dominant in the coarsening process.

If such a situation occurs, then during the annealing process voids will diffuse toward the step and coalesce with it. As a result of such a process, we will be left with a denuded zone with fewer voids around the step. One can use this width to get an estimate for the scale of all the diffusive scaling exponents of the clusters. We got much better results here than in the previous paper [13] for those values. One can also understand in some detail the difference between the upper and lower terrace relative to a step and the changes in the void densities there. One can also study the effect of hits of voids on the steps. The changing size of the voids will tend to create a more complicated scaling relation in the step correlations.

We experiment with a Si(111)7×7 surface with incomplete coverage that includes steps with an average distance of about 200 nm between them. Voids were formed on the terraces between the steps. When the sample is annealed, the following changes occur in the surface. The first one is the growth of the voids, which was already discussed in [13] and on which we will elaborate further as we continue in this paper. The second change is a dramatic growth in the step width, which is the fluctuation of the step coordinates from the straight mean direction. In Si(111)7×7, which is prepared at elevated temperatures, the steps are usually straight and oriented in the $(1,\bar{1},0)$ direction [20], although sometimes unit-cell-sized kinks can be observed [21]. Generally, one can detect almost no step width in such systems. A third exceptional feature is the existence of a denuded zone of voids near the step. This denuded zone grows in time and has some nonsymmetric aspects in its structure.

All these three features are consistent with a phenomenological description of diffusion of clusters in our system at a rate which is dependent on the size and the coalescence of these clusters with each other or with the step. We show in this paper how all the experimental details fit together.

Furthermore, using this information we can show that coarsening in this problem is dominated by diffusion-driven processes, and the dominant coarsening mechanism is coalescence.

We start our discussion in Sec. II with a description of the experiment and the measurement of step correlations and their basic explanation. In Sec. III we analyze the width of the denuded zone and derive the relevant growth exponents from it. In Sec. IV the shape correlations are explained theoretically and discussed from the experimental point of view. In Sec. V the denuded zone densities are analyzed in more detail, and in the final section we make final conclusions about this problem.

II. THE EXPERIMENT

Several STM studies on vacancy islands were performed [22–24]. Our experiments were performed with a custom-made STM with a level motion demagnifier [25]. It begins with a Si(111)7×7 surface on which amorphous silicon is deposited at room temperature to an extent that forms a coverage of 94%. After annealing the surface, 94% of it is covered by a crystalline layer while 6% is voids in this crystalline layer. In the beginning of the process, there are many randomly distributed small voids, which undergo a coarsening process as the sample is annealed. Figure 1 shows an image of an experiment in which the sample was annealed for 8 min to 600 °C. Most of the surface is in the 7×7 reconstruction, but it includes 5×5 reconstruction domains probably due to the release of strain in the surface as a result of the presence of the voids. Four voids with variable shapes and sizes are seen. A step edge is seen in the upper left part of the image. Several grain boundaries (marked by the arrows) connect the voids.

All these structural features may complicate the coarsening dynamics. Grain boundary diffusion can affect the coarsening, in a similar way to what happens in the process of sintering [26–28]. Grain boundaries may act as diffusion sinks or diffusion pipes. In addition, the grains undergo an independent coarsening process. An additional complication may arise due to the presence of different reconstructions in the surface. For example, in Fig. 1 there is a domain with a 5×5 reconstruction between three voids. It is clear that the reduced stability of this reconstruction will affect the coarsening dynamics. In this case, these voids will attract each other, just because of the presence of the 5×5 domain between them. The 5×5 boundary of the void will emit more

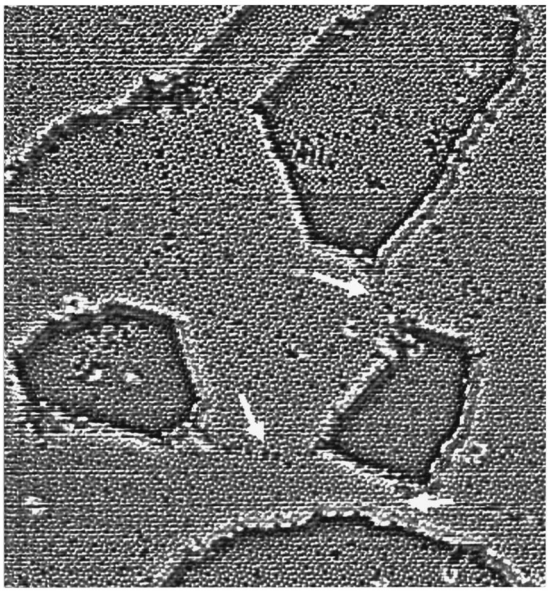

FIG. 1. An STM image of a Si(111)7×7 substrate after deposition of amorphous silicon at room temperature followed by annealing to 600 °C for 8 min. Area is $80\times80\,\mathrm{nm}^2$.

adatoms into the void than the 7×7 boundary. As a result, the void will migrate in the direction of the 5×5 boundary. In our ongoing theoretical discussion, we ignore these possible complications.

The steps that were observed in the experiments are much rougher than the steps normally observed in the Si(111) 7×7 surface. Moreover, it was easy to notice that the steps also become wider and more correlated as time goes on. In order to quantify the step coarsening, we have made a quantitative analysis of the roughness of the steps. In Fig. 2 we show an image which was observed after annealing a sample of 0.94 coverage of *a*-Si on Si(111)7×7 in 600 °C for 60 min. The image shows two terraces with many voids in each one (but more voids in the upper one). Also, the step looks much rougher than a normal step in Si(111)7×7. The accurate coordinates of the step can be measured and the results are plotted in the graph below the image as $h(x,t)$, where h is the height and x is a coordinate in the mean direction of the interface. Using such a result, we can analyze the step width and correlations. Interface correlations are defined as

$$c(y)=\langle[h(x)-h(x+y)]^2\rangle=y^{2\chi}, \tag{1}$$

where the $\langle\,\rangle$ sign is an average on x and χ is the roughness exponent. Figure 3 shows the curves calculated from steps in three times. An average of several steps is required in order to get meaningful data. The roughness curves for annealing times at 600 °C of 1, 30, and 60 min are shown from top to bottom, respectively. A clear biexponential behavior is observed. The roughness exponents for the lower scale are observed below a certain crossover scale $x=L_{\mathrm{co}}$, and is $\chi=0.8\pm0.05$. The values of the average void radius, for annealing times 1, 30, and 60 min, are 9, 11.5, and 13.5 nm, respectively, while the corresponding crossover scales are 5.8, 10.5, and 15 nm, respectively. The roughness exponent

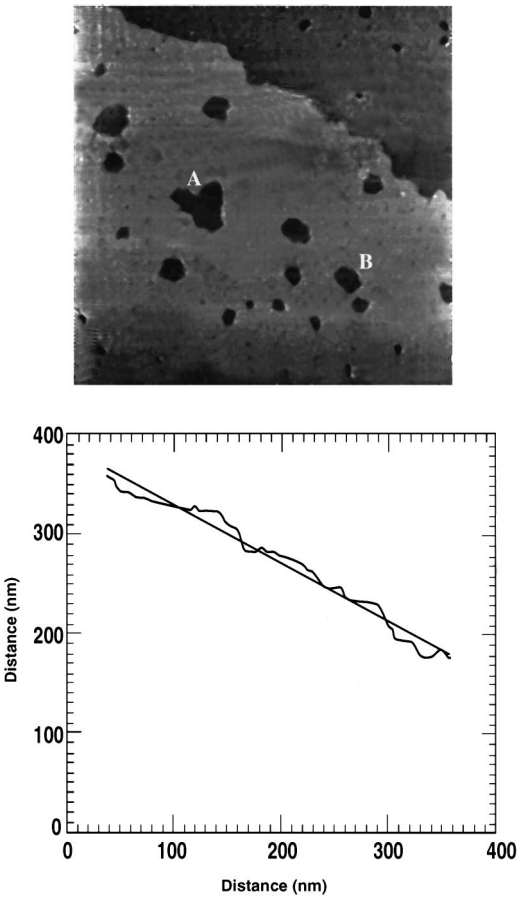

FIG. 2. An STM image of crystallized amorphous silicon after an annealing period of 60 min at 600 °C. The area is $180\times180\,\mathrm{nm}^2$. The multiple voids *A* and *B* are marked in the images.

in larger scales is $\chi=0.5\pm0.02$, which is the classical exponent for one-dimensional deposition of particles (voids in our case) [29,30].

III. INTERFACE DYNAMICS AND DENUDED ZONE

The only reasonable explanation for the connection between the coarsening of voids and the scaling of the roughness of the steps is that the lower scale is related to a deposition of voids on the step. So the range with the high exponent is related to the morphology of the voids and the standard scaling is on higher scales where a usual roughening process is activated. This is also in accord with the fact that the characteristic cutoff scale is very close to the average void scale.

As discussed earlier in the context of void coarsening [13], voids diffuse in this system and can hit the step and roughen it. A hit from the upper terrace direction creates a crater in the step which will relax in time. However, when a void will hit from the lower terrace direction, a different scenario will occur. Since the dominant dynamical effect is adatom release, adatoms from the step will move into the void, destroying it and again creating a crater in the step (not exactly in the same shape but in the same scale). In both cases the step velocity will be in the direction of the upper terrace.

So the basic dynamics on the interface is the addition of

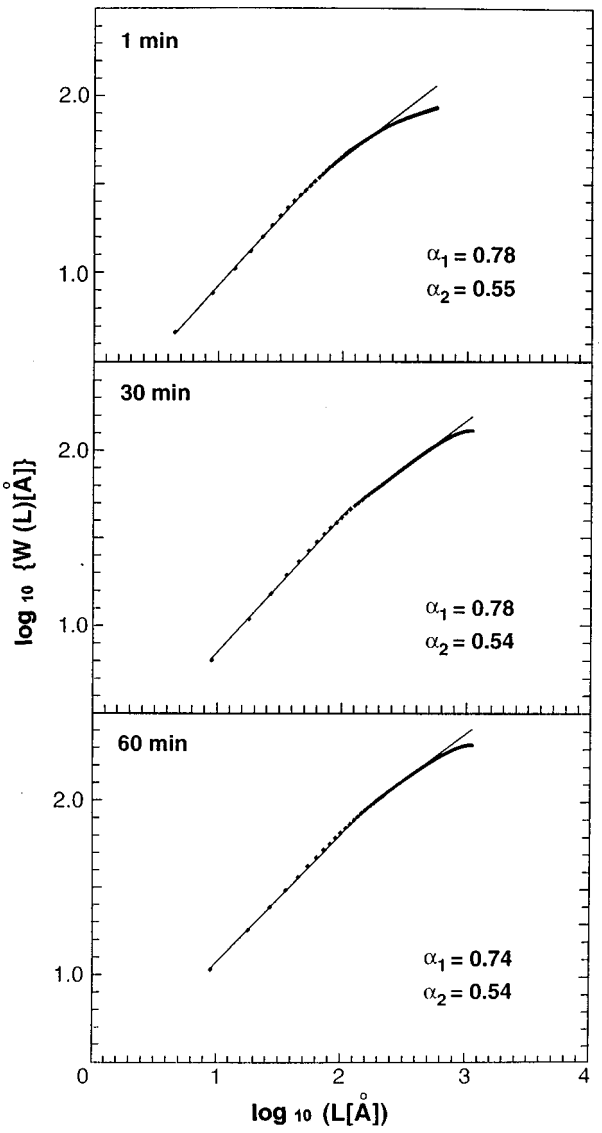

FIG. 3. Roughening curves from the steps in the images observed after annealing of 1, 30, and 60 min, respectively. The number of steps which were used for the calculation in these times was 7, 4, and 7, respectively.

voids. These voids hit the interface with a rate which is defined mainly by void diffusion and growth. Consider first a dynamical process in which voids of uniform size R hit a step. Below the scale R one would observe the scaling of the voids which is linear at low values. At larger scales one would observe a global scaling belonging to the equation that controls the interface dynamics [29]. In these scales the roughening exponent is $\chi=0.5$. Furthermore, if there is a distribution of sizes in R, the lower part will be modified. A growth in the characteristic size of the hitting voids $R\sim t^{\beta}$ will shift the crossover L_{CO} between the scalings to higher values of y.

Obviously the diffusion of voids towards the interface will create denuded zones in the upper and lower terraces. The rate at which voids hit the step is related to the growth of those denuded domains. For the sake of the scaling argument that is given here, we will assume that both scale as $x_d \sim t^d$. Since the integrated missing void area is proportional to x_d, the rate of hitting of voids on the step is

$$A(t)=t^c\sim t^{d-1}. \tag{2}$$

The physically reasonable model for void diffusion would be that c is related to the cluster diffusion exponent. If $D \sim R^{-l}$, the diffusion constant scales in time as $D\sim t^{-l\beta}$, where $\beta=(2+l)^{-1}$ [14]. The denuded zone is the voidless area in which most of the voids have already reached the step. It has a characteristic scale x_d, in the upper and lower terrace, which is determined by the simple diffusion equation

$$x_d^2=D(t), \tag{3}$$

so one gets

$$d=0.5(1-l\beta). \tag{4}$$

As stressed before, the void current exponent is proportional to $d-1$, so we get $c=-0.5(1+l\beta)$. c is negative and $c<-0.5$ ($c=-0.5$ is the result of a simple diffusive model). Note that since β is related to l, the exponent depends only on l. So, in principle, by measuring the width of the denuded zones one can estimate the values of l and β.

We now come back to the experiment to find those scales. The void area near the step was measured as a function of time and distance. We have separated the area in the upper and the lower terraces to stripes parallel to the steps, each stripe having a width of 20 nm, and we calculated the total area of voids in this stripe. The bin size of 20 nm is an optimal compromise between the better spatial resolution and the smaller relative errors. The error in the experiment was estimated as follows: Since the density of voids (Fig. 4) is defined as the ratio between the area of the voids within each stripe and the total area of the stripe, $\rho_v=A_v/A_{\mathrm{tot}} \sim N_v\overline{a}/A_{\mathrm{tot}}$, where N_v is the number of voids in the stripe and $\overline{a}$ is the average void area, the error in ρ_v is estimated as $\delta\rho_v\sim(N_v)^{0.5}/N_v$. The results are shown in Fig. 4 for three annealing times. It is important to remark that the errors far from the step are larger. This is due to the fact that the steps appear diagonal in our images, and A_{tot} of stripes far from the steps is, on the average, smaller. This is a result of the fact that the maximum scan range in our microscope is $360 \times 360\,\mathrm{nm}^2$.

There are some exceptional features in these results. The first is that we see a clear widening of the area without voids, but it is nonlinear in time. The second is the asymmetry in the distribution of voids in the upper and in the lower terrace near the step. This asymmetry is manifested in two effects. The first is a much larger width of the denuded zone in the lower terrace, and the second is a completely voidless area near the step in the lower terrace. These structural features will be studied in detail in Sec. V of this paper.

We first discuss the denuded zone growth exponent. Measuring the width of the denuded area in the three times (Fig. 4), we get the estimate $x_d\sim t^{0.2\pm0.03}$. Using Eq. (4) we get

$$l=3.0\pm0.4. \tag{5}$$

We can use this value to calculate the void growth exponent,

$$\beta=0.2\pm0.03, \tag{6}$$

and this coarsening is controlled by coalescence. The accuracy of this estimate is limited because of the fact that factors

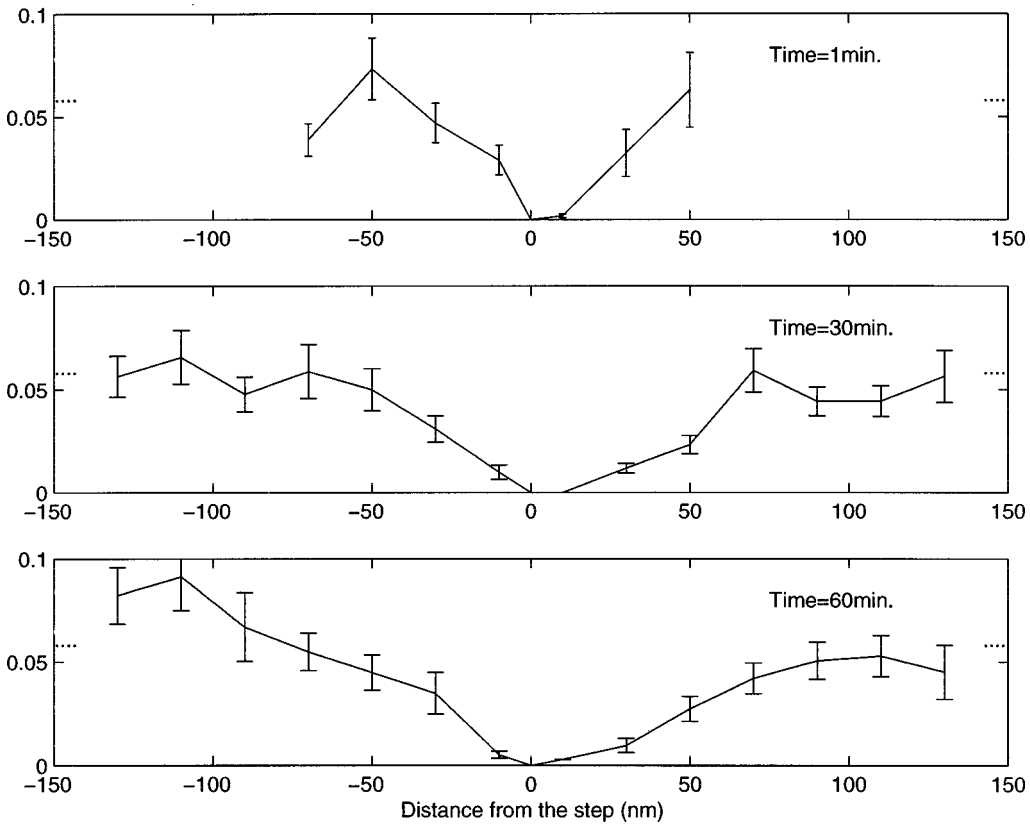

FIG. 4. Density of voids in the upper (left) and the lower (right) terraces as a function of the distance from the steps analyzed in Fig. 3. This is expressed as a fraction of the area that is covered with voids. The errors in these values were determined as described in the text.

between relative widths in different times should scale like the time ratios to the power of d. This is a rather small number for reasonable experimental times.

As we speculated in the previous paper, indeed the coarsening process in this system is not the standard diffusive Ostwald ripening. This is clearly seen by the nonstandard diffusive exponent, which scales like the periphery diffusion exponent ($D \sim R^{-3}$ [14–16]). So the coarsening in our case is driven by a diffusive coalescence mechanism.

IV. ANALYSIS OF INTERFACE DYNAMICS AND CORRELATIONS

We wish to consider a 1D step which is driven by additive noise, which is supposed to represent the hitting of voids with the predefined rates. Since the average void size goes up in time, we can assume that the noise correlation increases accordingly. We will assume the simplest step dynamics, which is the Edward Wilkinson dynamics (EW) [29],

$$\frac{dh(x,t)}{dt} = \nu \frac{d^2h(x,t)}{dx^2} + \eta(x,t). \tag{7}$$

The noise term $\eta(x,t)$ is supposed to represent the hitting of voids on the step. This noise term contains information about the void growth and the rate of the hitting of the step by the voids. At a certain time the probability to have a hit at a site is $t^{-c-\beta}$. To get the site correlations one has to multiply by R^2, so

$$\langle \eta(r)\,\eta(r)\rangle = t^{\beta-c}. \tag{8}$$

The correlation at a scale larger than some maximal time-dependent cluster size R vanishes. Since the average radius grows, we can assume.

$$\langle (\eta(r)\,\eta(r'))^2\rangle \sim t^{\beta-c} f((r-r'/R)), \tag{9}$$

where for $r-r' > R$ the correlation decays to zero. Generally, one can expand $f(r) = 1-r^2$ for small r. Since the EW equation is linear, it is convenient to write this type of correlation in Fourier space:

$$\langle \eta(k)\,\eta(k')\rangle = t^{\beta-c}\delta(k+k')g(kR). \tag{10}$$

We get the general expression

$$\langle h_k^2\rangle = \exp(k^2T)\int_0^T \exp(-k^2t)t^{\beta-c}g(kR(t))dt. \tag{11}$$

If $\beta < 0.5$ (as in our case), there are three dynamical regions in this problem: The first one is in scales above a large-scale cutoff, which is trivially defined in the EW equation as $1/k_0 \sim R_0 = T^{0.5}$. In this range one would get a constant scaling,

$$\langle h_k^2\rangle = T^{\beta-c+1}. \tag{12}$$

The width and $C(y)$ will be proportional to this number.

In an intermediate region $2\pi/R(t) < k_i < k_0$. The result of the h_k integration is simply

$$\langle h_k^2\rangle = t^{\beta-c+1}/k^2. \tag{13}$$

The final region where $1/k < R_c$ is more complicated. To analyze it, we assume that the final correlation $g(r/R_c)$ is dominant there. By fitting the scale at k_c to the scale in the previous equation, we get

$$C(y) = T^{1/2-c} y^2 \tag{14}$$

if $f((r-r')/R) - 1 \sim (r-r')^2$.

We performed a simulation of the EW equations with an assumption of $c=0$, $\beta=0.2$, and measured the correlation function $C(y,t)$ as a function of time and position. Indeed one observes three dynamical domains as are indeed found in the experiment.

From these results one can see that when $\beta - c + 1 < 0$, there will be a decay of the total width. A second obvious critical value is $c=0.5$. Above this value the correlations at the scale R_c will decay. So if the model becomes nonconservative, the total step scaling can even decrease as is indeed observed in simulations.

This indicates the existence of a critical exponent where the width will start going down. One can consider models with different dynamics and different relaxation rules like the Kardar-Parisi-Zhang (KPZ) equation. In those cases we expect that the critical exponents will be smaller.

A. The experimental correlations

We refer again to the measurement of the correlations in the experiment. We have three experimental points from which we can derive a set of values for the coarsening. We choose the following scales and estimate their relevant exponents: First, W_1, the width at the scale $x=1.0$; second, the scale L_{CO}; and third, the scale W_{CO} at the crossover scale. We now give their values at the times given in the preceding section. We find that

$$W_1 \sim t^{0.0+0.1}, \tag{15}$$

$$L_{\mathrm{CO}} \sim t^{0.2\pm0.1}, \tag{16}$$

$$W_{\mathrm{CO}} \sim t^{0.15\pm0.15}. \tag{17}$$

We should note that our ability to get more precise values is limited due to the small amount of voids that hit the interface.

An analysis of c using the denuded zone values [using Eq. (2) and the values of d we derived from the experiment] yields $c=-0.75\pm0.05$. This indicates according to the equation of the EW predictions that $W_{\mathrm{CO}}^2 \sim t^{-\beta-c+1}$. So the prediction is within our very limited experimental accuracy. The same thing applies to the scaling exponents of W_1 and L_{CO}.

V. THE GROWTH OF THE DENUDED ZONES

To understand the evolution in time of the denuded zones and the steps, let us discuss the equations of motion for the voids in the upper terrace and in the lower one. For the sake of this discussion we will assume a completely diffusive mechanism with no cluster growth. We define a void area density $\rho(y,t)$ as the average void area in distance y from the step. In the upper terrace we get a diffusion equation for the void density,

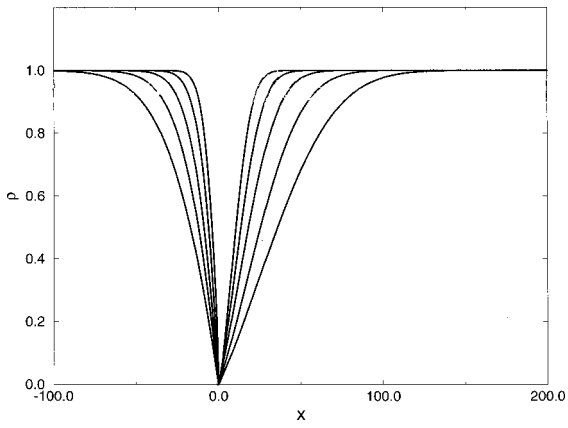

FIG. 5. We show a result of a simulation using the equations for the void density without interaction. In the figure we show the density in the upper (left part) and the bottom (right) terraces as a function of time at five consecutive times ($t=2^i$, $i=1,5$), where $D=1.0$ and $\rho(\infty)=1$ for the models. The fraction between the first width and the second is close to 2.

$$\dot{\rho}_u = D\rho_{u,yy}, \tag{18}$$

where ''y'' is a sign for differentiation, while in the lower terrace we will get

$$\dot{\rho}_l = D\rho_{l,yy}, \tag{19}$$

where we assign the sign u,l for the upper and lower terraces, and the D's should be the same. For the sake of this discussion, which is focused on the understanding of the zone asymmetry, we ignore the radius dependence of D. The boundary conditions for both void densities are

$$\rho(y_s) = 0.0, \tag{20}$$

where y_s is the moving position of the boundary, and

$$\rho(\pm\infty) = \rho_0. \tag{21}$$

Removal of atoms from the step results in a step velocity which can be estimated as

$$v_s = D[\rho_u(y_s) - \rho_l(y_s)]_y, \tag{22}$$

where y_s is the step position, $y_s = y_0 + \int v_s dt$. The interface moves in the direction of the upper terrace. The asymmetry between the lower and upper terrace is obvious, so it is clear that the lower terrace should be wider. Since the interface can only move because of voids that hit it, in long times $v_s = t^{-0.5}$ since the width of the deluded zone cannot grow in a faster rate than $t^{1/2}$.

One can solve these equations. In Fig. 5 we present the results of a simulation. One can clearly observe that the results are similar to the experimental results. The width in the upper terrace region [the place where $\rho(x)=0.5$] is half of the width in the lower terrace region, as is observed in the experiment. We think that this result lends strong support to our analysis.

To understand the dip in the density in the lower terrace, one has to consider another effect: the dynamics of the step. The merging of voids with the step creates a lot of sites where adatoms can easily be emitted. So the step emits adatoms as it relaxes. The details of this process can be quite elaborated since the detailed dynamics and interaction of the step are complicated.

We make a mean-field assumption that the step emits adatoms in an amount which is proportional to its velocity. These adatoms can be absorbed again in voids near the step or diffuse away. The mean-field effect of absorption in voids is a smaller density of matter of voids. Rewriting the previous equations, we have an additional adatom density $\rho_a(y,t)$ in the lower terrace. The equations of motion in the lower terrace are (the equations in the upper terrace are the same)

$$\dot{\rho}_a = D_a \rho_{a,yy} - A\rho_a\rho_l \tag{23}$$

and for ρ_l it is

$$\dot{\rho}_l = D\rho_{l,yy} - A\rho_a\rho_l . \tag{24}$$

The boundary conditions for the void densities are the same as before, and for ρ_a it is $\rho_a(\infty)=0$ and $\rho_a(y_s)_y = Cv_s$. We have two additional interaction constants. The first is the adatom diffusion constant D_a and the second is A. In principle, A can depend on both densities and diffusion constants. Since we cannot estimate A very well, we will just assume some value for A and D_a and show how the distribution is modified.

To capture some of the ingredients of the experiment, we assume that $D_a = 4D$ and $A = 20.0$. The resulting densities are given in Fig. 6. A first almost trivial result is that we observe a flattening of the lower density. A second result is that in time as distances become larger, the densities converge into the densities of the model without interactions. An estimate of a detailed picture of interaction and a more detailed theoretical analysis of the two previous models will be given elsewhere.

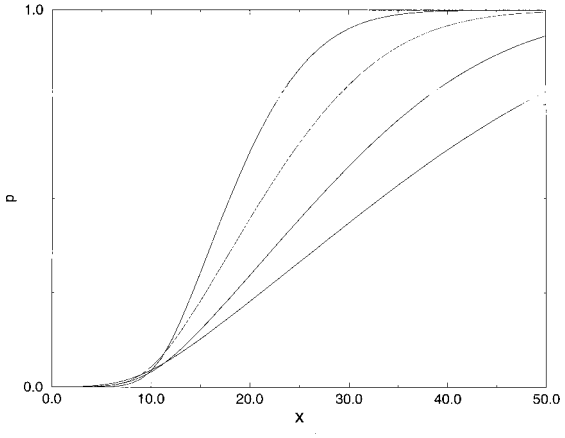

FIG. 6. Denuded zones with an interaction with adatoms. We give only the lower terrace. The flattening of the curve at early times is clearly seen. This feature disappears at long times.

VI. CONCLUSIONS

In this paper we showed that one can understand the coarsening of voids on a Si surface at 600 °C in a very detailed manner. The first point that we made here is that by using the measurement of the denuded zone, one can measure the scaling exponents of the diffusion constants and the growth of voids. As guessed in [13], voids indeed diffuse and coalesce and we were able to prove that this coarsening is dominated by this with a reasonable accuracy.

Furthermore, we were able to explain the shape of the denuded zone density by a simple model of interaction between voids and the step and we were even able to explain more complications using interactions with adatoms. The step morphology is defined by hits of the voids.

ACKNOWLEDGMENTS

This work was supported by the Minerva Foundation, Munich, Germany and the Basic Research Foundation administered by the Israeli Academy of Sciences and Humanities. One of us (Y.M.) is an incumbent of the Lilian and George Lyttle Career Development Chair.

[1] I. M. Lifshitz and V. V. Slyozov, J. Phys. Chem. Solids **19**, 35 (1961).
[2] C. Wagner, Z. Elektrochem. **65**, 581 (1961).
[3] G. Binnig, H. Rohrer, C. Gerber, and E. Weibel, Phys. Rev. Lett. **49**, 57 (1982).
[4] G. Binnig, H. Rohrer, C. Gerber, and E. Weibel, Phys. Rev. Lett. **50**, 120 (1983).
[5] G. Binnig, C. F. Quate, and C. Gerber, Phys. Rev. Lett. **56**, 930 (1986).
[6] H. P. Lang, V. Thommen-Geiser, and H. J. Guentherodt, Synth. Met. **77**, 161 (1996).
[7] E. Ter-Ovanesyan, Y. Manassen, and D. Shachal, Phys. Rev. B **50**, 8020 (1994); Isr. J. Chem. **36**, 45 (1996).
[8] L. Vazquez, R. C. Salvarezza, P. Ocon, P. Herrasti, J. M. Vara, and A. J. Arvia, Phys. Rev. E **49**, 1507 (1994).
[9] R. Q. Hwang, J. Schroeder, C. Guenther, and R. J. Behm, Phys. Rev. Lett. **67**, 3279 (1991).
[10] W. Ostwald, Z. Phys. Chem., Stoechiom. Verwandtschaftsl. **34**, 495 (1900).
[11] J. A. Marqusee, J. Chem. Phys. **81**, 976 (1984); J. A. Marqusee and J. Ross, J. Phys. Chem. **80**, 536 (1984); M. Marder, Phys. Rev. Lett. **55**, 2953 (1985); Q. Zheng and J. D. Gunton, Phys. Rev. A **39**, 4848 (1989); P. W. Vorhees, G. B. McFadden, R. F. Boisvert, and D. I. Meiron, Acta Metall. **36**, 207 (1988).
[12] Y. W. Mo, J. Kleiner, M. B. Webb, and M. G. Lagally, Phys. Rev. Lett. **66**, 1998 (1991); J. A. Strocio and D. T. Pierce, Phys. Rev. B **49**, 8522 (1994); W. Theis, N. C. Bartelt, and R. M. Tromp, Phys. Rev. Lett. **75**, 3328 (1995).
[13] E. Ter-Ovanesyan, Y. Manassen, N. Ramesh Rao, and Z. Olami, J. Vac. Sci. Technol. B **15**, 1317 (1997).
[14] D. S. Scholl and R. T. Scodje, Phys. Rev. Lett. **75**, 3158 (1995).

[15] A. F. Voter, Phys. Rev. B **34**, 6819 (1986).
[16] J.-M. Wen, S.-L. Chang, J. W. Burnett, J. W. Evans, and P. A. Thiel, Phys. Rev. Lett. **73**, 2591 (1994).
[17] W. W. Pai, A. K. Swan, Z. Zhang, and J. F. Wendelken, Phys. Rev. Lett. **79**, 3210 (1997).
[18] A. V. Latyshev, A. B. Krasilnikov, and A. L. Aseev, Phys. Status Solidi A **146**, 251 (1994).
[19] H. Watanabe and M. Ichikawa, Phys. Rev. B **54**, 5574 (1996).
[20] R. S. Becker, J. A. Golovchenko, E. E. McRae, and B. B. Swartzentruber, Phys. Rev. Lett. **55**, 2028 (1985).
[21] G. Wilhelmi, T. Kampschulte, and H. Neddermeyer, Surf. Sci. **333-333**, 1408 (1995).
[22] P. Bedrossian and T. Klitsner, Phys. Rev. Lett. **68**, 646 (1992).
[23] X.-S. Wang, R. J. Pechman, and J. H. Weaver, Appl. Phys. Lett. **65**, 2818 (1992).
[24] J. de la Figuera, J. E. Prieto, C. Ocal, and R. Miranda, Solid State Commun. **89**, 815 (1994).
[25] J. E. Demuth, R. J. Hamers, R. M. Tromp, and M. E. Welland, IBM J. Res. Dev. **30**, 396 (1986).
[26] S. M. Allen and J. W. Cahn, Acta Metall. **27**, 1085 (1979).
[27] M. P. Anderson, D. J. Srolovitz, G. S. Grest, and P. S. Sahni, Acta Metall. **32**, 783 (1984).
[28] W. Y. Shih, W.-H. Shih, and I. A. Aksay, J. Mater. Res. **10**, 1000 (1995).
[29] T. Halpin-Healy and T. Zhang, Phys. Rep. **254**, 216 (1995); A. L. Barbasi and H. E. Stanley, *Fractal Concept in Surface Growth* (Cambridge University Press, Cambridge, 1995).
[30] F. Wu, S. G. Jaloviar, D. E. Savage, and M. G. Lagally, Phys. Rev. Lett. **71**, 4190 (1993).